International Journal of Applied Earth Observations and Geoinformation 95 (2021) 102257

Contents lists available at ScienceDirect

International Journal of Applied Earth Observations and Geoinformation

journal homepage: www.elsevier.com/locate/jag

Impact of the number of dates and their sampling on a NDVI time series reconstruction methodology to monitor urban trees with Venμs satellite

Carlos Granero-Belinchon [a,b,*], Karine Adeline [a], Xavier Briottet [a]

[a] ONERA-DOTA, University of Toulouse, FR-31055 Toulouse, France
[b] IMT Atlantique, Lab-STICC, UMR CNRS 6285, F-29238 Brest, France

ARTICLE INFO

Keywords:
Time series reconstruction
Urban environment
Venμs
NDVI
Trees

ABSTRACT

This article studies the influence of the number of satellite remote sensing acquisition dates and their sampling on the performance of a time series reconstruction method developed in Granero-Belinchon et al. 2020. This method initially aimed at monitoring urban London plane (*Platanus x acerifolia*) trees, and was tested with Sentinel-2 imagery at spatial resolutions of 10 and 20 m and a temporal revisit of 5 days. Due to its higher revisit frequency of 2 days while having a similar spatial resolution of 10 m, Venμs imagery was consequently used in the present article to fulfill with the purpose of this study. The strategy relies on the building of different acquisition date configurations based on the Venμs time series by considering uniform and non-uniform samplings and with a total number of acquisitions ranging from 45 to 14. Thus, the aim of the article is to examine the number of annual acquisitions needed to describe properly a vegetation phenological cycle and the impact of the annual sampling of these acquisitions on the final reconstructed time series. To this end, this study was carried out by using the widely used Normalized Difference Vegetation Index (NDVI). Results showed that on one hand, applied on an acquisition configuration composed of at least 18 uniformly sampled dates throughout the year, this reconstruction methodology is able to describe correctly the annual NDVI dynamics but leads to inaccuracies in the description of intra-annual ones. Nevertheless, these intra-annual descriptions are improved with the increase of the number of acquisitions. On the other hand, strongly non-uniform acquisition date samplings lead to inaccurate descriptions of the undersampled time periods but correct descriptions of the rest of the time series curve. The study case is London planes located in Toulouse (France) with 45 cloud-free Venμs images during the year 2019. Finally, this work emphasizes the main limitations of the studied reconstruction methodology when few acquisitions or very non-uniform acquisition date samplings are available and thus the identification of borderline cases in future applications and other study cases.

1. Introduction

Urban trees are beneficial for urban ecosystems (Alexandre, 2013; Hassan and Lee, 2015; Manning, 2008) since they provide shadows (in the case of Paris 3% of the city surface is shaded by urban trees (Rol-Tanguy et al., 2010)), influence urban temperatures (urban cool islands) and increase the air quality of the city (Vos et al., 2013; Alavipanah et al., 2015), refix CO_2 from fossil fuel consumption (Chaturvedi et al., 2013) and contribute to biodiversity conservation (Chaturvedi et al., 2013). In particular, London planes (*Platanus x acerifolia*) are frequently used in European cities such as Madrid, London, Toulouse or Brussels, where they are planted in rows along avenues, rivers and canals. However, urban environments are unfavourable for trees development because of restricted root space availability, air pollution, soil nutrient deficiency and a insufficient water drainage (Krizek and Dubik, 1987). Furthermore, since the middle of the 20th century, the canker stain disease of London plane spreads over Europe (Anselmi et al., 1994; Panconesi, 1999) leading to an increase of tree mortality for this species.

Among the approaches to characterize vegetation greening dynamics, satellite remote sensing is a widely used candidate since it gives access to image acquisitions with high frequency and covering large areas such as the entire urban pattern from the downtown to the peri-urban or rural environments. Thus, it has proved to be an adapted technique to study urban vegetation communities and to deliver a complete diagnostic over the entire city (Granero-Belinchon et al., 2020; Zipper et al., 2016; Zhou et al., 2016). Then, the vegetation phenology is

* Corresponding author at: IMT Atlantique, Lab-STICC, UMR CNRS 6285, F-29238 Brest, France.
E-mail address: carlos.granero-belinchon@imt-atlantique.fr (C. Granero-Belinchon).

https://doi.org/10.1016/j.jag.2020.102257
Received 3 April 2020; Received in revised form 1 October 2020; Accepted 20 October 2020
Available online 9 November 2020

monitored from the use of Vegetation Indices (VI) time series derived from remote sensing imagery (Zhang et al., 2003; Vrieling et al., 2018). Actually, the annual phenology, which mainly depends on the climate seasonal variations and the specific vegetation species, controls the vegetation dynamics. Four main phenological phases can be distinguished in deciduous trees such as London planes: Greenup, Maturity, Senescence and Dormancy periods (Zhang et al., 2003; Seyednasrollah et al., 2019).

However, the characterization of urban vegetation from remote sensing is still challenging due to: (1) the high manmade and natural material heterogeneity beneath tree vegetation, (2) the 3D structures inducing shadows on tree vegetation, (3) the small sizes of urban vegetated areas, (4) the large number of species composing each vegetated zone … All these characteristics have to be considered to study urban vegetation and require a high spatial resolution.

Hence, new generation satellites such as Venμs and Sentinel-2 (S-2) reveal to be adapted to the study of vegetation dynamics since they are able to measure Normalized Difference Vegetation Index (NDVI) at 10 m and with revisit times of 2 and 5 days respectively. Presently, Venμs has the best temporal repetitivity at the desired spatial resolutions of 10 m if compared to the other existing satellites. In addition, London planes in rows, due to their large sizes (tree crown diamaters around tens of meters, tree heights exceedings 20 m, and rows of hundred of meters), reduce mixed pixel effects (due to shadows and background), and can be studied as a single species vegetation from satellite remote sensing. The limited Ground Sampling Distance (GSD) of Sentinel-2 and Venμs in regard to the London plane crown size is partially overcame by the row configuration.

In order to correctly study vegetation dynamics from remote sensing, time series reconstruction methodologies are frequently used on NDVI time series to reduce noise induced by atmospheric, viewing angle or cloud cover variabilities between dates (Viovy et al., 1992; Beck et al., 2006; Chen et al., 2004; Vrieling et al., 2018; Yang et al., 2019). In urban environments, the importance of co-registration variability between dates in the noise of the raw time series has been also shown (Granero-Belinchon et al., 2020). Consequently, reconstruction methodologies have been developed to obtain NDVI time series which can be used to study the vegetation greening and its dynamics (Granero-Belinchon et al., 2020; Wang et al., 2016; Menzel et al., 2006; Wielgolaski, 1999). However, NDVI time series reconstruction methods were initially designed for sensors with extremely high revisit frequencies (at least one acquisition per day) and moderate spatial resolutions (hundred of meters), such as MODIS and AVHRR (Viovy et al., 1992; Beck et al., 2006; Chen et al., 2004). These methods were later extended to satellites such as Sentinel-2 with better spatial resolutions but lower revisit frequencies (Vrieling et al., 2018; Yang et al., 2019). But then some questions arise: how many annual acquisition dates are required to properly describe a phenological cycle? What is the impact of the annual sampling of these acquisitions on the final reconstructed time series? Do these lower revisit frequencies allow you to observe intra-annual events? Some of these questions have been already studied for reconstruction methodologies applied on MODIS (Zhang et al., 2009), but also on Sentinel-2 over rural areas (Vrieling et al., 2018; Zhou et al., 2012). However, in the case of high spatial resolution satellites with lower temporal revisit frequencies, the impact of the number of acquisitions and their sampling on reconstruction methods should be examined in detail, and especially for urban environments where these studies are still non-existent.

Recently a new time series reconstruction methodology to monitor urban trees was developed to be applied on high spatial resolution satellite imagery with high revisit frequency such as Sentinel-2 and Venμs (Granero-Belinchon et al., 2020). In addition, its performance to characterize different NDVI time series dynamics of London planes located at different environments in Toulouse, France, from 2018 Sentinel-2 images (20 images) has been shown. As a continuation of this previous work (Granero-Belinchon et al., 2020), this article proposes to study the robustness of this methodology on (1) the time sampling and (2) the decrease of the number of dates composing the raw time series, when reconstructing the NDVI curve of Toulouse London planes. To this end, a raw NDVI time series with a high number of acquisitions is needed. Thus, Venμs, with a revisit time of 2 days, provided 45 cloud free images of Toulouse during 2019 (more than the double of the number of images used in the previous study with Sentinel-2 Granero-Belinchon et al., 2020), which reveals to be a good initial raw time series candidate to be undersampled through various ways. As such, different configurations of acquisition dates can be derived and their influences on the time series reconstruction final product can be analysed.

This article is structured in 4 sections. Section 2 presents first, the study area and the Venμs image properties, and second, the methodology used in this article (time series reconstruction, sampling strategies and evaluation criteria). In Section 3, the results are shown and discussed. Finally, Section 4 presents some conclusions and perspectives.

2. Materials and methods

2.1. Study area

Toulouse is a French city located in the south-west, close to the Pyrenees mountains, between Atlantic ocean and Mediterranean sea. With around 500.000 inhabitants, it is the fourth largest city of France, see Fig. 1. Its weather is characterized by a humid temperate climate favouring vegetation development. Toulouse is crossed by the Garonne river and by “Canal de Midi” and “Canal de Brienne” artificial canals. London planes are found in large avenues in the city center, but also along the river and the canals. In this work, we focused on London planes growing along the “Canal de Brienne”, see Fig. 2. These old London planes are located near the city center and the orientation of their rows is north-west, with two rows of trees (one at each side of the canal) and crown diameters between 10 and 20 m (crown sizes are not homogeneous). In addition, these London planes are generally higher than the surrounding buildings.

2.2. Satellite remote sensing data

Venμs is a Visible Near-InfraRed (VNIR) multispectral Israeli-French mission with 12 spectral bands. It was launched in August 2017 and provides one image of Toulouse every 2 days with a spatial resolution of 10 m (Ferrier et al., 2010). Its viewing angle is almost constant across the year with a viewing zenith angle of $\theta_z^v \approx 31^\circ$ and a viewing azimuth angle of $\phi_a^v \approx 182^\circ$. In Toulouse, the solar angles (zenith θ_z^i and azimuth ϕ_a^i angles) at Venμs aquisition time (≈11:00 local time) varies along the year from $\theta_z^i \approx 165^\circ$ and $\phi_a^i \approx 65^\circ$ during winter to $\theta_z^i \approx 145^\circ$ and $\phi_a^i \approx 25^\circ$ during summer (Granero-Belinchon et al., 2020).

THEIA platform (https:www.theia-land.fr) gives free access to Venμs Bottom Of Atmosphere reflectance (level 2A) processed images of Toulouse. Moreover, THEIA delivers co-registered images (maximum co-registration errors of 60% of the pixel size are allowed), with cloud masks, and both quality and atmospheric information. For 2019, which is the first year for which THEIA provides images covering the whole year, 45 Venμs images of Toulouse are available (images with strong cloud coverage, higher than 50% or without the study area, were not considered).

2.3. Methods

The procedure used to analyse the impact of the number of dates and their sampling on the Granero-Belinchon et al. 2020 time series reconstruction methodology (Granero-Belinchon et al., 2020) was based on three main steps: (1) from a reference acquisition set composed of 45 cloud free Venμs images, different samplings were performed to generate new sets with less acquisitions, (2) the studied reconstruction

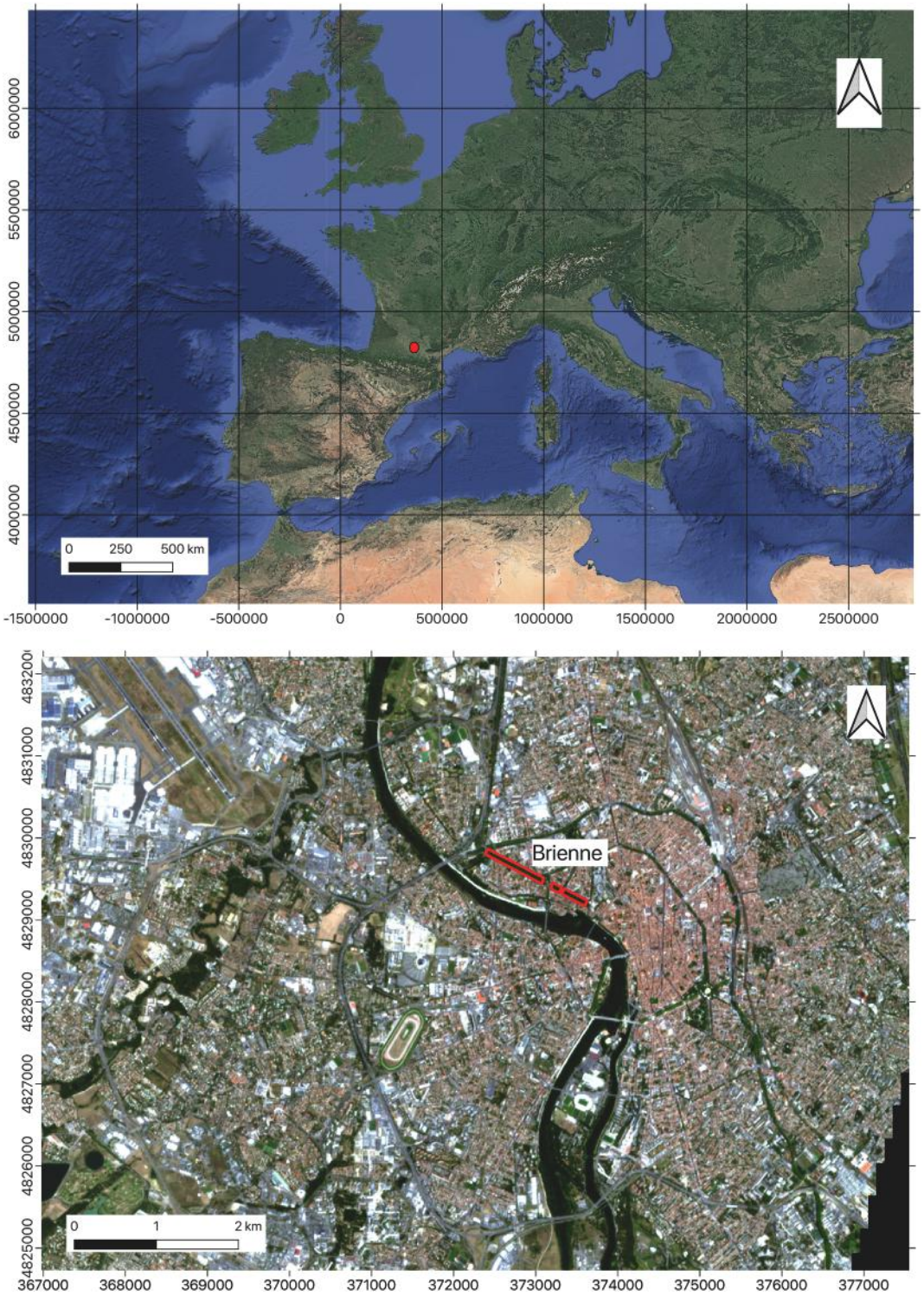

Fig. 1. Top: Google Satellite image of Europe. The red dot indicates the location of Toulouse. Bottom:Venμs Red-Green-Blue (RGB) composite image of Toulouse (France). The delineated area corresponds to the London plane rows along the Canal de Brienne (red). (For interpretation of the references to color in this figure legend, the reader is referred to the web version of this article.)

methodology was applied on the reference set (where all cloud-free images were used) and on each new generated set, and (3) the similarity between the reference reconstructed time series and the reconstructed time series from the different sampling configurations was evaluated with assessment metrics, see Fig. 3.

2.3.1. Time series reconstruction

The time series reconstruction methodology used to analyse NDVI dynamics of urban trees, presents four steps:

(1) A manual masking aims at delimiting the vegetation study area. This mask was visually delineated on Venμs images, see Fig. 2,

Fig. 2. Toulouse (France) Canal de Brienne study area. Top: Venμs RGB composite image. The delineated area corresponds to the London plane rows along the Canal de Brienne (red). Bottom: Google-Earth image. (For interpretation of the references to color in this figure legend, the reader is referred to the web version of this article.)

(2) NDVI was calculated for each pixel of the masked area and for all the available dates of the year for a given acquisition dataset,
(3) Then, an unsupervised classification based on a pixel by pixel weighted iterative fitting of raw NDVI time series was applied. Thus, pixels for which the error fit was small were considered as vegetation pixels. The double-logistic function was chosen to fit NDVI time series (Beck et al., 2006; Vrieling et al., 2018),
(4) A weighted iterative Savitzky-Golay filtering (Chen et al., 2004) was applied on pixels classified as vegetation in order to obtain the final NDVI time series. Its mean over the vegetation pixels of

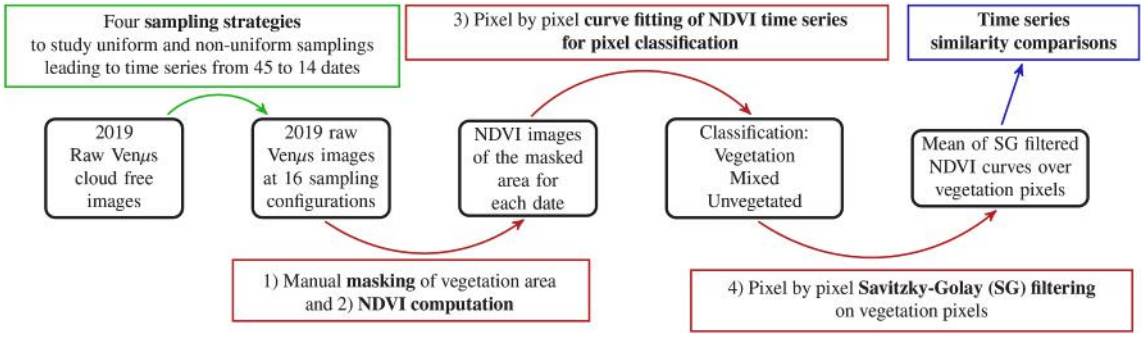

Fig. 3. Proposed methodology to characterize the impact of time sampling on NDVI time series reconstruction. Red squares describe the time series reconstruction methodology, the green square the sampling strategies and the blue square the evaluation criteria. Black squares indicate the outcomes of the different steps. (For interpretation of the references to color in this figure legend, the reader is referred to the web version of this article.)

the masked area was then used to represent the greening behavior of the vegetation group.

While the masks were manually built from QGIS software, the NDVI estimation, the double-logistic fit and the Savitzky-Golay filter come from our own implementation in python 3.6. For this purpose, three main python libraries were used: SciPy, NumPy and Gdal. A detailed description of the methodology can be found in Granero-Belinchon et al. 2020 (Granero-Belinchon et al., 2020).

2.3.2. Sampling strategies

In order to study the impact of the number of available dates on the time series reconstruction methodology, 4 sampling strategies, with a total of 16 different time configurations, were considered and applied on the reference 45 cloud-free 2019 Venus time series. This process provides new acquisition datasets with a number of dates varying between 14 and 45 and including uniform and non-uniform samplings. In addition, some of these configurations simulate the lost of a whole period of the year approximately corresponding to a phenological phase. The four sampling strategies were the following:

(1) The complete set of Venμs images with 45 dates was undersampled by only retaining one over two dates by starting either on the first or the second date of the annual time series. This procedure provides two uniform undersampled time series with 22 and 23 dates, which in this article were called "Odd" and "Even" respectively. This strategy allowed to study the impact of reducing the number of available dates to a half but maintaining an uniform sampling.
(2) From the previous "Even" undersampled time series, five and nine dates were randomly eliminated following three different random combinations, thus providing three time series with 18 dates and three time series with 14 dates respectively. These time series simulate cases with a very reduced number of available dates over the year.
(3) The undersampling removed a complete phenological period. This step provided 4 strongly non-uniform undersampled time series where Greenup, Maturity, Senescence and Dormancy phenological periods were one by one absent, leading to acquisition datasets composed of 38, 37, 39 and 37 dates respectively. Depending on the meteorological conditions and the satellite revisit times, phenological periods can be frequently lost or at least poorly sampled over a given study area. This strategy also allowed to study the impact of strongly non-uniform samplings.
(4) The dates from Toulouse Venμs 2019 time series which are closer to the Toulouse Sentinel-2 cloud-free passing dates from 2017, 2018 and 2019 (THEIA datasets), were used to create three new Venμs subsampled time series with respectively 15, 20 and 22 dates (corresponding to the number of Sentinel-2 acquisitions for 2017, 2018 and 2019). Actually, using the 2017–2018–2019 Sentinel-2 passing dates over Toulouse allowed to study real configurations adapted to Toulouse meteorology (sampling could be non-uniform and in some cases a whole phenological period could be poorly sampled).

2.3.3. Evaluation criteria

To evaluate how the different time series configurations impact the time series reconstruction, three global indicators were selected: (1) the number of pixels classified as vegetation in the reconstruction methodology, (2) the Root Mean Square Error (RMSE) and (3) the Spectral Angle Mapper (SAM) (Kruse et al., 1993).

$$RMSE = \sqrt{\frac{\sum_{i=1}^{N}\left(\widehat{NDVI}_i - NDVI_i\right)^2}{N}} \quad (1)$$

$$SAM = \cos^{-1}\frac{\sum_{i=1}^{N}\widehat{NDVI}_i\, NDVI_i}{\sqrt{\sum_{i=1}^{N}\widehat{NDVI}_i^{\,2}}\sqrt{\sum_{i=1}^{N}NDVI_i^2}} \quad (2)$$

with N the number of acquisitions, $\widehat{NDVI}_i$ the estimated NDVI value for acquisition i on the newly undersampled time series and $NDVI_i$ the NDVI value of acquisition i estimated on the reference time series. Only acquisitions appearing in both time series are used in the comparison. Both RMSE and SAM were estimated between the reconstructed time series with 45 dates used as the reference, and the other reconstructed time series from the studied configurations. Thus, they differently characterized the annual similarity between the reference and the studied case. While RMSE measures a time average of the exact NDVI difference between curves, SAM does not take into account NDVI offsets. In addition, to complete those annual descriptions a fourth indicator, (4) the NDVI difference between the reference and the studied configurations, was considered to observe intra-annual deviations.

The first evaluation criteria (the number of pixels classified as vegetation) will verify if a statistical analysis can be performed on the NDVI time series representing the vegetation group (to reduce size effects in the statistical study a large enough dataset is required). The two global evaluation criteria, RMSE and SAM, are classical statistical tests to characterize the similarity between time series (Lhermitte et al., 2011). Finally, the NDVI difference is not a global criteria and so it emphasizes punctual differences between time series that can be of importance for short term phenological events. All these evaluation criteria were estimated using our own implementation in Python 3.6 and the Python package NumPy.

3. Results and discussion

3.1. 2019 Venμs reference time series

Fig. 4(a) shows the reference Venμs NDVI time series of Brienne London plane rows for 2019, which contains 45 dates. In this figure, four phenological periods can be distinguished: (1) Dormancy, characterised by an almost flat behavior with small NDVI values around 0.5 and covering mainly winter season, (2) Greenup, characterised by a sharp increase of NDVI from 0.5 to 0.85, and occurring during spring, (3) Maturity which presents the highest NDVI with values between 0.79 and 0.91 and occurring in summer, and (4) Senescence which presents a sharp decrease of NDVI from Maturity values to Dormancy ones. In addition, two intra-annual events which are identified by sharp decreases of NDVI (Granero-Belinchon et al., 2020) can be observed on this reconstructed NDVI time series: the first between Day of Year (DoY) 160 and 195, and the second between DoY 210 and 290 (dashed red vertical lines), with a total decrease in NDVI of 0.05 and 0.1 respectively. One can remind that classical reconstruction methodologies such as double-logistic or double-hyperbolic-tangent function fitting can not describe intra-annual events, oppositely to the method used in this study. Then, the temporal repartition of Venμs acquisitions is quite uniform along the year, except marginally in the Dormancy and Senescence periods. The mean sampling distance between 2019 Venμs images is 7.4 days. However, this averaged sampling distance depends on the phenological period corresponding to: 10 days during Dormancy, 6.8 days during Greenup, 5.7 days during Maturity and 11.6 during Senescence.

3.2. Uniform sampling with more than 20 dates

Fig. 4(b) shows on the one hand the reconstructed NDVI time series of "Even" (23 samples) and "Odd" (22 samples) undersamplings with the reference time series for visual comparison. While the annual behaviour is well described by both "Even" and "Odd" curves (see global evaluation criteria results in Table 1), differences appear in the description of the intra-annual events. "Even" time series perfectly describes the intra-annual event starting at DoY 210 but seems to erase the intra-annual event starting at DoY 160. On the other hand, "Odd" time series slightly describes the intra-annual event starting at DoY 160 but smoothes the one starting at DoY 210. The differences between the reference and these undersampled time series are also shown in Fig. 4 (b). They quantify the NDVI deviations due to a decreasing number of dates in the time series. Results showed that the largest deviations for both "Even" and "Odd" undersampled time series are smaller than 0.05 NDVI.

Table 1
Venμs time series analyzed configurations together with the number of dates of each configuration, the number of pixels classified as vegetation and the evaluation criteria used to evaluate the similarity between the reference time series and the other configurations over the whole year. For RMSE and SAM, mean values are shown with the corresponding standard deviations between brackets.

Configuration	# dates	# vegetation pixels/ total # of pixels	RMSE (NDVI)	SAM (Radians)
Reference	45	448/923	0	0
Even	23	385/923	0.06 (0.03)	0.04 (0.02)
Odd	22	567/923	0.05 (0.02)	0.03 (0.01)
18 dates random 1	18	259/923	0.07 (0.03)	0.05 (0.02)
18 dates random 2	18	426/923	0.06 (0.03)	0.04 (0.01)
18 dates random 3	18	426/923	0.06 (0.03)	0.04 (0.01)
14 dates random 1	14	193/923	0.09 (0.05)	0.06 (0.02)
14 dates random 2	14	177/923	0.1 (0.05)	0.07 (0.02)
14 dates random 3	14	557/923	0.06 (0.02)	0.05 (0.01)
Greenup missing	38	390/923	0.06 (0.03)	0.04 (0.02)
Maturity missing	37	549/923	0.05 (0.02)	0.03 (0.02)
Senescence missing	39	415/923	0.05 (0.03)	0.04 (0.01)
Dormancy missing	37	635/923	0.04 (0.02)	0.02 (0.01)
Sentinel-2 2017 configuration	15	613/923	0.05 (0.02)	0.04 (0.01)
Sentinel-2 2018 configuration	20	691/923	0.04 (0.02)	0.03 (0.01)
Sentinel-2 2019 configuration	22	442/923	0.05 (0.02)	0.04 (0.01)

The first and second columns of Table 1 provide the sampling configuration and the number of dates of each studied case. In addition,

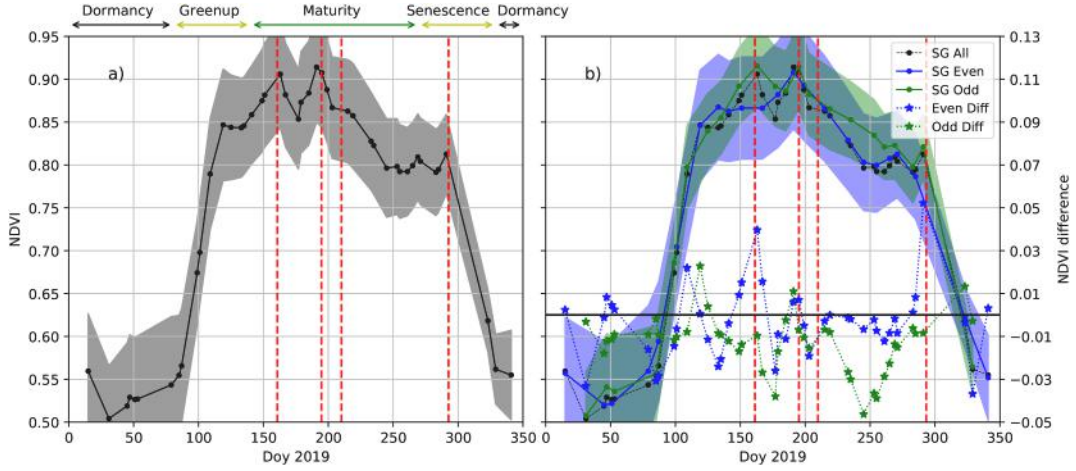

Fig. 4. 2019 Venμs NDVI reconstructed time series with (a) all the 45 dates and (b) the 23 "Even" dates (blue) and the 22 "Odd" dates (green). The NDVI standard deviation is indicated with shaded areas. In (b) NDVI reference reconstructed time series is plotted in black for comparison, and the differences between this reference and the "Even" and "Odd" reconstructed NDVI time series are plotted in dashed blue and dashed green respectively. Dashed red vertical lines indicate the start and the end of the two intra-annual periods of NDVI dynamics. (For interpretation of the references to color in this figure legend, the reader is referred to the web version of this article.)

its third column provides the number of pixels classified as vegetation by the methodology. Finally, Table 1 also quantifies the annual similarity between the different studied cases and the reference with the RMSE and the SAM criteria. For these three cases, "Reference", "Even" and "Odd", the number of pixels classified as vegetation varies between 41% for "Even" and 61% for "Odd", compared to 48% for the reference. In addition, "Odd" being closer to the reference during Greenup and Senescence, and better describing the first intra-annual event, presents slightly lower RMSE and SAM values (RMSE = 0.05 NDVI and SAM = 0.03 radians), compared to "Even" (RMSE = 0.06 NDVI and SAM = 0.04 radians).

From the above results, we can state that the annual NDVI behavior can be still well described with 22 and 23 dates uniformly sampled. However, this decrease in the number of dates, even with uniform samplings, leads to less performant descriptions of intra-annual events, resulting in the lost or hide of at least one of the observed intra-annual periods. These results also show the sensitivity of the reconstruction methodology to the specific acquisitions, since two raw NDVI time series with almost the same number of dates uniformly sampled lead to different reconstructed curves. The specific available acquisitions especially impact the curve fitting step (see Section 2.3). As explained in Granero-Belinchon et al. 2020, the classification is based on a double-logistic curve fitting with a threshold on the fitting error (Granero-Belinchon et al., 2020). Consequently, the number of samples of the time series influences the fit performance: undersampled time series will be worse fitted. However, another important factor to take into account in this classification procedure is the similarity of the fitted time series to a double-logistic curve. Importantly marked intra-annual events such as the one appearing at DoY 160 make time series be far from a double-logistic behavior and then they increase the fit error. Thus, the fitting error that determines the classification will depend on the specific acquisitions defining the raw curve, and then, the pixels classified as vegetation will depend on these specific acquisitions, influencing the final reconstructed time series.

3.3. Uniform sampling with less than 20 dates

Fig. 5(a) shows three NDVI time series when 18 different random dates are used. In these cases the annual behavior is well described but deviations can be found in the start of the NDVI rise (corresponding to the start of the greenup) and the NDVI fall (corresponding to the start of the senescence). Moreover, the first intra-annual event is not described by these time series. This is not the case of Fig. 5(b) where three NDVI time series having 14 different random dates are shown. When only 14 dates remain, the two intra-annual periods are lost. In addition, strong differences all along the year can also be noticed with high deviations reaching until 0.1 NDVI.

Table 1 shows that the number of pixels classified as vegetation when the number of dates is strongly decreased dropped and achieved at minimum 19–20% (14 dates random 1 and 2). It also points out an increase in annual dissimilarities with RMSE values reaching at maximum 0.1 NDVI (14 dates random 2) and SAM values reaching at maximum 0.07 radians (14 dates random 2). In addition, annual dissimilarity as measured by RMSE and SAM tends to be higher for 14 dates time series than for 18 dates ones, with a global increase around 0.03 NDVI for RMSE and 0.02 radians for SAM.

NDVI time series with 18 dates and uniform sampling are still able to define the annual NDVI behavior and some important intra-annual events. On the other hand, NDVI time series with 14 dates and uniform sampling does not describe intra-annual events and can present strong deviations with respect to the reference. Then, we can state that 18 dates are enough to characterize the annual NDVI behavior, while reconstructed time series with 14 dates can not be used to characterize NDVI dynamics with our methodology.

3.4. Non-uniform sampling with the lost of a phenological period and more than 30 dates

Fig. 6 shows the reconstructed time series when a whole phenological period is lost (in any case more than 37 dates remain) with the reference for visual comparison. We can observe that loosing a phenological period mainly influences the NDVI time series description of the lost period, without influencing the description of the rest of the time series, where only small differences are found. In detail, when Greenup is lost the time series difference reaches 0.08 NDVI during Greenup, but only 0.01 NDVI on the other phenological periods. Similarly when Senescence is lost, NDVI difference reaches 0.11 during Senescence, with losses of less than 0.02 on the other periods. In addition, when Maturity and Dormancy are lost, a constant slight shift of the NDVI time series to upper values is observed on the rest of the reconstructed phenological periods: about 0.01 NDVI when Maturity is lost and between 0.01 and 0.03 NDVI when it is Dormancy.

Table 1 shows a number of pixels classified as vegetation oscillating between 42% when Greenup is absent to 69% when Dormancy is absent, while RMSE values range between 0.06 NDVI (Greenup lack) and 0.04 NDVI (Dormancy lack) and SAM values between 0.04 radians (Greenup and Senescence) and 0.02 radians (Dormancy).

Loosing a whole phenological period still accurately preserves the

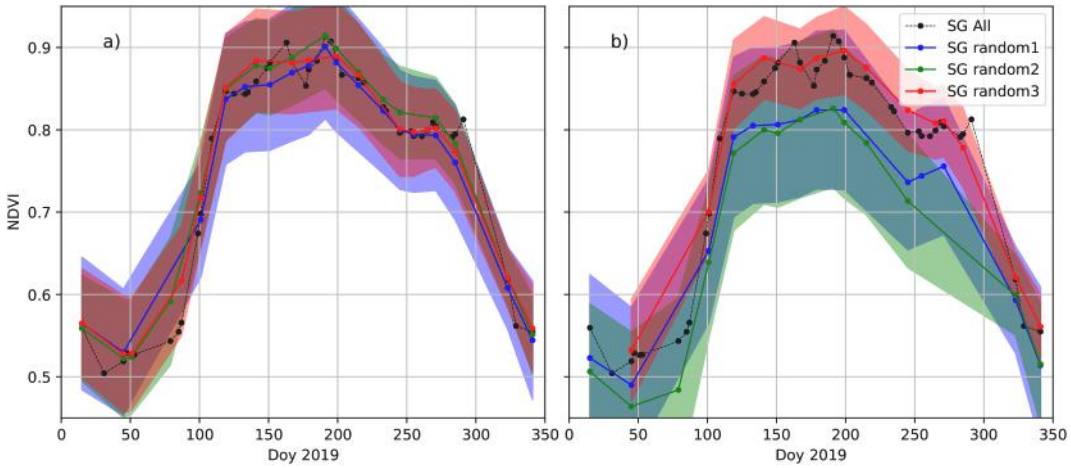

Fig. 5. 2019 Venμs NDVI reconstructed time series with (a) 18 random dates and (b) 14 random dates. Blue, green and red lines represent three different random combinations of samples. The NDVI standard deviation is indicated with shaded areas. Reference NDVI reconstructed time series is plotted in black for comparison. (For interpretation of the references to color in this figure legend, the reader is referred to the web version of this article.)

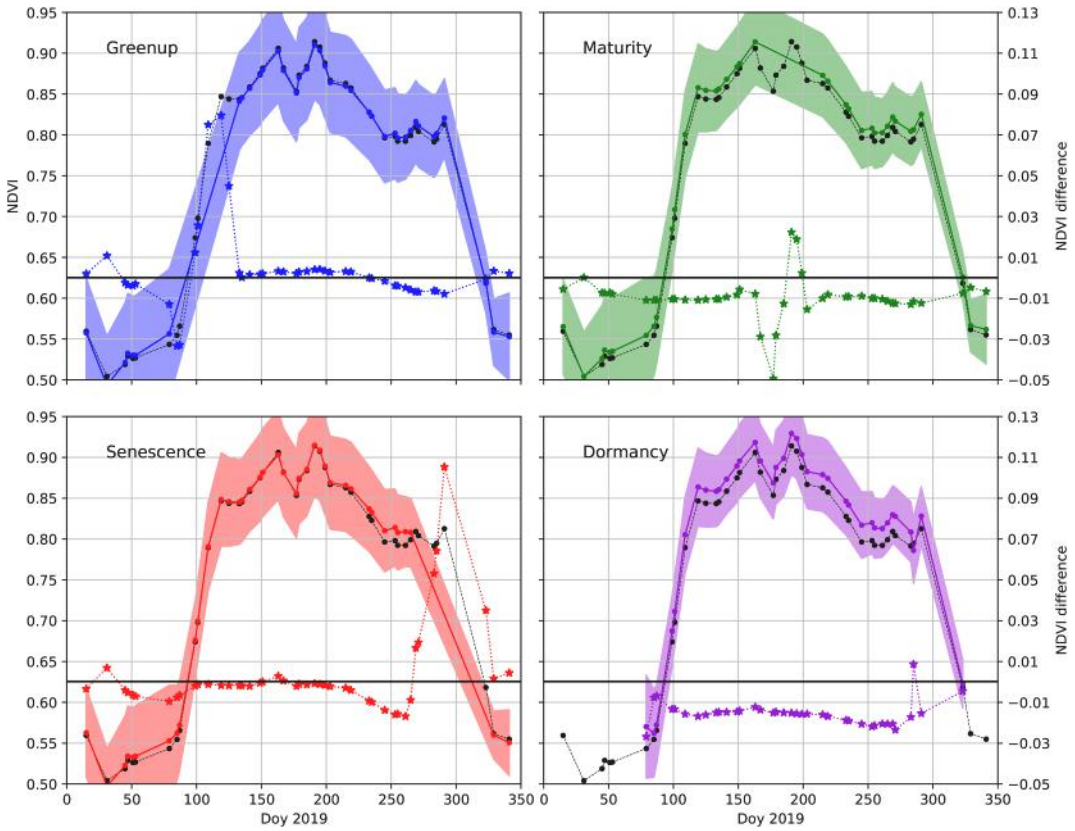

Fig. 6. 2019 Venμs NDVI reconstructed time series without Greenup dates in blue, Maturity dates in green, Senescence dates in red and Dormancy dates in purple. The NDVI standard deviation is indicated with shaded areas. Reference NDVI reconstructed time series is plotted in black for comparison and the difference between this reference and the undersampled reconstructed NDVI time series is plotted in dashed colour line. (For interpretation of the references to color in this figure legend, the reader is referred to the web version of this article.)

whole behavior of the NDVI time series except for the lost period, where the description is non existent. In addition, RMSE and SAM seem to indicate that loosing Greenup or Senescence impacts more the annual description that loosing Maturity or Dormancy.

3.5. Non-uniform sampling with less than 20 dates adapted to match 2017–2018–2019 Sentinel-2 cloud-free acquisition DoYs

In order to study the influence of having a few number of acquisitions (between 15 and 22) with non-uniform sampling on the NDVI time series reconstruction methodology, we decided to set a time configuration in agreement with the meteorological conditions of Toulouse. Hence, we kept the 2019 Venμs acquisitions at DoYs closer to those of Sentinel-2 acquisitions for the years 2017, 2018 and 2019, which present 15, 20 and 22 dates respectively. This leads to the reconstruction of hypothetical NDVI time-series obtained by Venμs, if the 2019 Venμs data had been acquired at the Sentinel-2 intervals of 2017, 2018 and 2019. The mean difference between Sentinel-2 acquisition DoYs and the used Venμs ones is 2 days, with a maximal difference of −13 days during the senescence period of 2017. In agreement with previous results, Fig. 7(a) shows that 15 samples does not allow to describe neither intra-annual events, nor maximal NDVI values. In addition, since the Greenup phase is lost, large deviations are also noticed in the Spring description. Fig. 7(b) and (c) illustrate better annual descriptions of the NDVI time

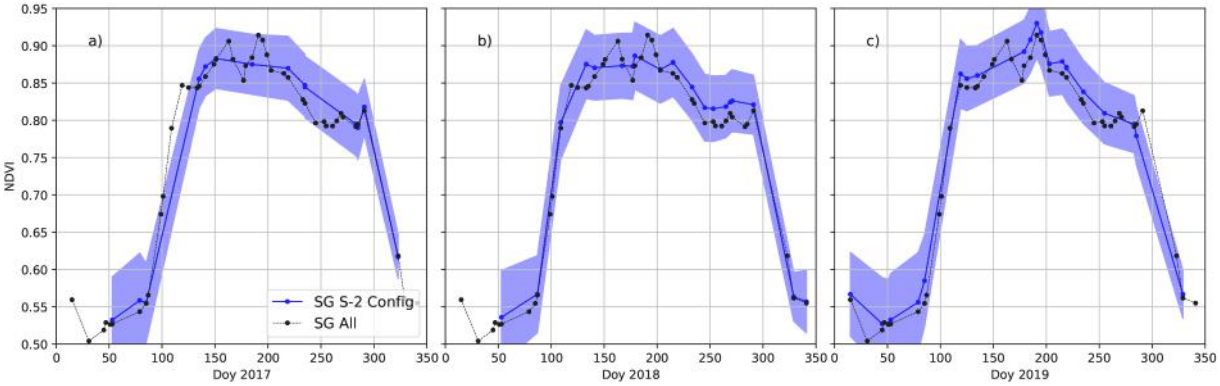

Fig. 7. 2019 Venμs NDVI reconstructed time series with (a) Sentinel-2 2017 time sampling configuration, (b) Sentinel-2 2018 time sampling configuration and (c) Sentinel-2 2019 time sampling configuration. The NDVI standard deviation is indicated with shaded areas. Reference NDVI reconstructed time series is plotted in black for comparison.

series, notably for Dormancy, Greenup and Senescence periods. In the Maturity period both figures characterize the intra-annual event starting at DoY 210 but they loose the one at DoY 160. Furthermore, the NDVI time series of Fig. 7(b) underestimates the maximal NDVI values, while that of Fig. 7(c) presents a good estimation.

For these three cases, the number of pixels classified as vegetation varies between 50% for the 2019 configuration to 75% for the 2018 configuration, see Table 1. RMSE values are between 0.04 and 0.05 NDVI and SAM values around 0.03–0.04 radians.

These results support the previous ones: (1) with 15 or less dates the description of the NDVI time series is not enough accurate since the intra-annual events are lost and the annual description introduces strong deviations. However with 20 and 22 time samples, reliable annual descriptions seem to be better obtained.

4. Conclusions

The main goal of this article is to evaluate the impact of the number of available acquisitions and their sampling on the NDVI time series reconstruction methodology from (Granero-Belinchon et al., 2020). The case study is the Toulouse urban London planes in rows from Canal de Brienne. With this purpose and from a whole set of Venμs acquisitions (45 dates during 2019), four different undersampling strategies are used: (1) reducing the number of dates by a half keeping a uniform sampling (one over two acquisitions are retained), (2) some acquisitions are randomly (with uniform distribution) removed until fewer than 20 dates are preserved, (3) loosing all the acquisitions from a whole phenological period (4 sets are generated where Greenup, Maturity, Senescence and Dormancy are respectively absent) and (4) Venμs acquisitions closer in DoY to Sentinel-2 acquisitions from 2017, 2018 and 2019 are used to build hypothetical Venμs time-series, with 15, 20 and 22 non-uniformly sampled acquisitions respectively. This allows to study real time configurations in agreement with Toulouse meteorology. In any case, the Venμs NDVI time series with 45 dates is used as reference for comparison, since it is supposed to better describe the NDVI time series curve.

It is shown that at least 18 acquisitions uniformly sampled are needed to describe the annual behavior of the NDVI time series. However, to do so for intra-annual periods more dates are required. Even with 22–23 acquisitions uniformly sampled, the methodology has shown limitations to characterize all the intra-annual periods appearing in the 45 acquisitions time series. Furthermore, loosing a whole phenological period if the rest of the time series is well sampled mainly influences the time series description of the lost phenological period, while it correctly describes the rest of the time series. Finally, studying the three time series generated according to Sentinel-2 2017, 2018 and 2019 acquisitions DoYs allows to corroborate previous results and to show the applicability of the time series reconstruction methodology on Sentinel-2 time series. Nevertheless, Sentinel-2 imagery has slightly higher co-registration errors (between 0.3 and 1.2 pixels) than Venμs (0.3 pixels), and then reducing the number of acquisitions during the year can have a more important influence on the Sentinel-2 time series reconstruction.

Thus, the main application of this work is the study and identification of borderline cases on which the studied reconstruction methodology (Granero-Belinchon et al., 2020) can present drawbacks when monitoring urban London planes in rows with Venμs satellite.

As a perspective to analyse these influences directly on Sentinel-2 data, other cities should be studied where: (1) a large number of Sentinel-2 acquisitions are available (due to the low cloud cover rate of the city), and (2) where large rows of London planes (or similar size trees) can be found. In addition, a complete study on the influence of the number of processed pixels on the methodology robustness should be performed in order to be able to apply this methodology in smaller urban tree species such as lime trees or chinaberry trees, or in smaller groups of trees as they can be found in other cities. Finally, the robustness of the reconstruction methodology should be also characterized on tree species with different greening behaviors, or for the same tree species when trees are found in other climate zones (impacting NDVI time series evolution across the year).

CRediT authorship contribution statement

Carlos Granero-Belinchon: Conceptualization, Methodology, Software, Validation, Formal analysis, Investigation, Writing - original draft, Writing - review & editing. **Karine Adeline:** Conceptualization, Methodology, Investigation, Writing - review & editing, Funding acquisition. **Xavier Briottet:** Conceptualization, Methodology, Investigation, Writing - review & editing, Funding acquisition.

Declaration of Competing Interest

The authors declare that they have no known competing financial interests or personal relationships that could have appeared to influence the work reported in this paper.

Acknowledgments

This research was funded by ONERA contract number 30221001F2019. The APC was funded by ONERA DOTA. The authors wish to thank THEIA platform for providing the needed Venμs processed images (Level 2A) and for stimulating discussions. The authors wish to thank A. Rolland and R. Binet from CNES for stimulating discussions on the radiometric and geometric quality of Venμs images. Finally, the authors want to thank ONERA for funding this research.

References

Alavipanah, S., Wegmann, M., Qureshi, S., Weng, Q., Koellner, T., 2015. The role of vegetation in mitigating urban land surface temperatures: a case study of Munich, Germany during the warm season. Sustainability 7 (4), 4689–4706.

Alexandre, F., 2013. The role of vegetation in the urban policies of european cities in the age of the sustainable city. Eur. Spatial Res. Policy 20 (2), 11–26.

Anselmi, N., Cardin, L., Nicolotti, G., 1994. Plane decline in european and mediterranean countries: associated pests and their interactions. EPPO Bull. 24 (1), 159–171.

Beck, P., Atzberger, C., Hogda, K., Johansen, B., Skidmore, A.K., 2006. Improved monitoring of vegetation dynamics at very high latitudes: a new mothod using MODIS NDVI. Remote Sens. Environ. 100, 321–334.

Chaturvedi, A., Kamble, R., Patil, N., Chaturverdi, A., 2013. City-forest relationship in Nagpur: one of the greenest cities of India. Urban Ofrestry Urban Greening 12 (1), 79–87.

Chen, J., Jonsson, P., Tamura, M., Gu, Z., Matsushita, B., Eklundh, L., 2004. A simple method for reconstructing a high-quality ndvi time-series data set based on the savitzky-golay filter. Remote Sens. Environ. 91, 332–344.

Ferrier, P., Crebassol, P., Dedieu, G., Hagolle, O., Meygret, A., Tinto, F., Yaniv, Y., Herscovitz, J., 2010. VENμS (Vegetation and Environment monitoring on a New MicroSatellite). In: Proceedings of IGARSS, IEEE International Geoscience and Remote Sensing Symposium, Honolulu, Hi, USA.

Granero-Belinchon, C., Adeline, K., Lemonsu, A., Briottet, X., 2020. Phenological dynamics characterization of alignment trees with Sentinel-2 imagery: a vegetation indices time series reconstruction methodology adapted to urban areas. Remote Sens. 12 (4), 639.

Hassan, A., Lee, H., 2015. Toward the sustainable development of urban areas: an overview of global trends in trials and policies. Land Policy 48, 199–212.

Krizek, D., Dubik, S., 1987. Influence of water stress and restricted root volume on growth and development of urban trees. J. Arboric. 13 (2), 47–55.

Kruse, F.A., Lefkoff, A.B., Boardman, J.W., Heidebrecht, K.B., Shapiro, A.T., Barloon, J. P., Goetz, A.F.H., 1993. The spectral image processing system (SIPS): Interactive visualization and analysis of imaging spectrometer data. Remote Sens. Environ. 44 (2–3), 145–163.

Lhermitte, S., Verbesselt, J., Verstraeten, W.W., Coppin, P., 2011. A comparison of time series similarity measures for classification and change detection of ecosystem dynamics. Remote Sens. Environ. 115, 3129–3152.

Manning, W., 2008. Plants in urban ecosystems: essential role of urban forests in urban metabolism and succession toward sustainability. Int. J. Sustain. Develop. World Ecol. 15, 362–370.

Menzel, A., Sparks, T., Estrella, N., Koch, E., Aasa, A., Ahas, R., Alm-Kübler, K., Bissolli, P., Braslavska, O., Briede, A., Chmielewski, F., Crepinsek, Z., Curnel, Y., Dahl, A., Defila, C., Donnelly, A., Filella, Y., Jatczak, K., Mage, F., Mestre, A., Nordli, O., Penuelas, J., Pirinen, P., Remisova, V., Scheifinger, H., Striz, M., Susnik, A., van Vliet, A., Wielgolaski, F., Zach, S., Zust, A., 2006. European

phenological response to climate change matches the warming pattern. Glob. Change Biol. 12 (10), 1969–1976.
Panconesi, A., 1999. Canker stain of plane trees: a serious danger to urban plantings in Europe. J. Plant Pathol. 81 (1), 3–15.
Rol-Tanguy, F., Alba, D., Dragoni, M., Minassian, H.T., Blancot, C., 2010. Essai de bilan sur le developpement des arbres d'alignement dans paris, Tech. rep. Atelier Parisien d'Urbanisme (APUR).
Seyednasrollah, B., Young, A., Hufkens, K., Milliman, T., Friedl, M., Frolking, S., Richardson, A., 2019. Tracking vegetation phenology across diverse biomes using version 2.0 of the PhenoCam Dataset. Sci. Data 6, 222.
Viovy, N., Arino, O., Belward, A., 1992. The Best Index Slope Extraction (BISE): A method for reducing noise in NDVI time-series. Int. J. Remote Sens. 13, 1585–1590.
Vos, P., Maiheu, B., Vankerkom, J., Janssen, S., 2013. Improving local air quality in cities: to tree or not to tree? Environ. Pollut. 183, 113–122.
Vrieling, A., Meroni, M., Darvishzadeh, R., Skidmore, A., Wang, T., Zurita-Milla, R., Oosterbeek, K., O'Connor, B., Paganini, M., 2018. Vegetation phenology from sentinel-2 and fields cameras for a Dutch barrier island. Remote Sens. Environ. 215, 517–529.
Wang, R., Cherkauer, K., Bowling, L., 2016. Corn response to climate stress detected with satellite-based NDVI time series. Remote Sens. 8 (4), 269.
Wielgolaski, F., 1999. Starting dates and basic temperatures in phenological observations of plants. Int. J. Biometeorol. 42, 158–168.
Yang, Y., Luo, J., Huang, Q., Wu, W., Sun, Y., 2019. Weighted double-logistic function fitting method for reconstructing the high-quality sentinel-2 ndvi time series data set. Remote Sens. 11, 2342.
Zhang, X., Friedl, M.A., Schaaf, C.B., Strahler, A.H., Hodges, J.C.F., Gao, F., Reed, B.C., Huete, A., 2003. Monitoring vegetation phenology using MODIS. Remote Sens. Environ. 84 (3), 471–475.
Zhang, X., Friedl, M.A., Schaaf, C.B., 2009. Sensitivity of vegetation phenology detection to the temporal resolution of satellite data. Int. J. Remote Sens. 30 (8), 2061–2074.
Zhou, J., Jia, L., Hu, G., Menenti, M., 2012. Evaluation of Harmonic ANalysis of Time Series (HANTS): impact of gaps on time series reconstruction. In: 2012 Second International Workshop on Earth Observation and Remote Sensing Applications, pp. 31–35.
Zhou, D., Zhao, S., Zhang, L., Liu, S., 2016. Remotely sensed assessment of urbanization effects on vegetation phenology in China's 32 major cities. Remote Sens. Environ. 176, 272–281.
Zipper, S.C., Schatz, J., Singh, A., Kucharik, C.J., Townsend, P.A., Loheide, S.P., 2016. Urban heat island impacts on plant phenology: Intra-urban variability and response to land cover. Environ. Res. Lett. 11, 054023.